

**RESEARCH
ARTICLE**

Which Kind of and How Much Disruption to the Symmetry of Double-Slit Is Necessary for the Fringe Pattern Changes Conjectured to Have Seemingly Manifested Psychophysical Faculty?

Daqing Piao

daqing.piao@okstate.edu

<https://orcid.org/0000-0003-0922-6885>

School of Electrical and Computer Engineering
Oklahoma State University
Stillwater, Oklahoma

SUBMITTED February 4, 2022
ACCEPTED June 2, 2022
PUBLISHED December 30, 2022

<https://doi.org/10.31275/20222533>

PLATINUM OPEN ACCESS



Creative Commons License 4.0.
CC-BY-NC. Attribution required.
No commercial use.

HIGHLIGHTS

A new study suggests that it could take no more than 10 picowatts (a picowatt is one millionth of one millionth of one watt) of power for matter to be affected by the human mind.

ABSTRACT

Identifying the most plausible cause of the fringe pattern changes in the double-slit of psychophysical domain (Radin et al., 2012, 2013) not only is instrumental to the understanding of the nature of psychophysical effects that may manifest but also will shed light on the effecting mechanism of such anomalous faculty should it be quantifiable. We implement computer simulations of double-slit fringe patterns based on the Huygens–Fresnel principle using the primary experimental geometrical parameters of Radin et al. (2013) to assess how an asymmetry of the double-slit configuration could affect the fringe visibility. The main result is that the normalized interference fringe corresponding to an asymmetry of the electrical field magnitude of 3/1 or 1/3:1 as was modeled by Radin et al. (2013) is grossly indifferent from that caused by an asymmetry of the spectral bandwidth of 0.00205 nm between the two slits at 632.8 nm center wavelength. A spectral broadening of 0.00205 nm of the light for the experimental setting utilized by Radin et al. (2013) could correspond to a power change of no more than 10 picowatts. Further studies are warranted to test this hypothesis towards understanding the nature of psychophysical faculty as was conjectured with Radin’s double-slit experiments.

KEYWORDS

Double-slit experiments, mind–matter, psychophysical faculty, asymmetry, psychophysical reality, transduction of energy, psychophysical effects, double-slit interference fringe patterns, spectral bandwidth, photonic properties, phase sensitivity,



1. INTRODUCTION

Psychophysical phenomena of various scales have been investigated by many laboratories over nearly a century's span using contemporary scientific instruments and statistical methodologies (Pratt, 1949; Rhine 1963; Schmidt, 1973; Tart et al., 1980; Jahn, 1982; Radin, 1982; Utts, 1986; McConnell, 1989; Dunne & Jahn, 1992; Bierman, 1996; Alexander, 2019; Giroladini & Pederzoli, 2021). However, the lack of a plausible physical mechanism to account for the intriguingly exhibited mind-matter interaction has prevented psychophysical research from being well-regarded by the physical science community (Shewmaker & Berender, 1962; Jamali et al., 2019; Tremblay, 2019; Walleczek & von Stillfried, 2019). Irrespective of the discipline, what physical science concerns would rest eventually on the transformation or transduction of energy between two different forms or states that may manifest as the change of a measurable physical property. For a phenomenon that does not result in a measurable change of any physical property, perhaps no psychophysical effects could be speculated about. On the other hand, however, one might encounter measurable changes of a specific physical property of which the cause could not be attributed unambiguously to a single factor or a specific pathway of affecting between an identifiable cause and an observable effect. Such uncertainty in terms of the explicability could be particularly intractable to the experiments of psychophysical essence.

In the optical domain, the diffraction pattern is substantiated by the phase behavior of light being a wave. Since the phase of light is sensitive to a length-change or an energy-variation or a power-shift corresponding to a sub-wavelength scale, the fringe pattern formed specifically by interferometric configuration that helps magnify the differential phase distribution or variation of the light field has allowed investigating phenomena that are too subtle to be measured by other means (Yacoby et al. 1994; Sztul & Alfano, 2006; Gachet et al., 2010; Lee et al., 2013). The extremely high sensitivity of interferometry has been taken advantage of in the pursuit of macroscopically quantifiable experimental demonstration of psychophysical faculties (Nelson et al., 1981, Jahn, 1982). Unfortunately, until a causally plausible mechanism in terms of the time-invariability and perhaps an intention-invariability could be entertained, or the role of mind in physics can be untangled (Klein & Cochran, 2017), changes of physical properties registered by instruments assumed to have evinced psychophysical faculty will remain controversial (Tremblay, 2019; Walleczek & von Stillfried, 2019), as they would be fundamentally difficult to replicate (Piao, 2021) due to the inability to apply adequate control of experi-

mental conditions—which arguably is the inevitable outcome of incomplete knowledge with regard to what those conditions really are.

As early as 1981, a Fabry-Perot interferometer illuminated by an incoherent light source (diffuse sodium lamp focused by a lens system) was implemented to test the possibility of psychophysical influence on altering the interference fringe patterns (Nelson et al., 1981). The engagement of a light source with high spatial and temporal coherence such as a laser, has allowed resolving fringe pattern variations at much higher fringe resolution or phase sensitivity than would be possible by using incoherent light sources. Following those early investigations based on interferometry, Radin et al. (2012, 2013, 2016) reported on variations in the interference fringe patterns in laser-engaged double-slit interferences. The fringe patterns in those studies were reported to have degraded in the fringe visibility which occurred in neurophysiological conjunction with an application of intention by a subject. The degradation of the visibility of the interference fringe from its baseline corresponded to a comparative reduction of the double-slit spectral power to its single-slit spectral power, which was conjectured to have manifested psychophysical influence since no other factors could be attributed to it (Radin et al., 2012). In accounting for the observation of the fringe visibility change, Radin et al. applied the Fraunhofer model of far-field light distribution to double-slit interference by considering that the light passing through the two slits could have esoterically reached an asymmetry due to psychophysical influence. Quantitatively, a 3:1 asymmetry of the electrical field magnitude of light between the two slits was demonstrated to be able to produce changes to the interference fringe with the fringe visibility close to that registered experimentally.

This present work puts forward an alternative model-interpretation of the reported change of fringe-visibility of the double-slit interference of Radin et al. We theorize that a change to the double-slit interference fringe pattern at the level reported by Radin et al. could very well, or highly more likely be caused by, a slight asymmetry of the spectral bandwidth of the light passing the two slits. This result could shed novel insights on the esoteric features of the conjectured psychophysical influence on double-slit interference.

Realizing this, we implemented computer simulations based on the Huygens-Fresnel principle using the primary geometrical parameters of the double-slit experiments of Radin et al. to assess how an asymmetry of the two slits in either a physical dimensional property or a photonic/spectral property would alter the interference fringe pattern. For fringe patterns that may be grossly difficult to differentiate based on the fringe visibility alone, Fourier

transformation of the fringe pattern is conducted to infer differences or deviations from the baseline that otherwise might be subtle.

The rest of this paper is structured as follows: **Section 2** outlines the gross geometry of the double-slit as well as the general approach of discretization for the computer simulation. **Section 3** details the asymmetries configured for the double-slit for assessing the effect of each kind of asymmetry on the fringe pattern. Asymmetries to the double-slit are introduced by changing the physical length-dimensional properties or photonic/spectral properties of one slit. Section 3 then presents the simulated outcomes of the double-slit interference fringe patterns for the asymmetries specified. When prompted, Fourier transform of fringe patterns associated with a specific asymmetry is conducted to examine the similarity of the power spectrum with the experimental data reported by Radin et al. An outcome of the computer simulation is cross-examining the analytical modeling of Radin et al. in terms of the effect of an asymmetry of the electrical field magnitude of 3:1 and 1/3:1 between the two slits. A fringe pattern of near-identical fringe visibility is produced by introducing an asymmetry in the electrical field magnitude (1/2:1, 1/3:1, 1/4:1, 1/5:1, and 1/6:1) and implementing an asymmetry on the spectral bandwidth (0.0017, 0.00205, 0.00223, 0.0037, and 0.0047 nm). **Section 4** discusses the power changes necessary for two specific conditions of asymmetry that are shown to produce fringe patterns grossly indifferent in terms of the visibility, one has an asymmetry of 1/3:1 on the electrical field magnitude akin to that modeled by Radin et al. and the other has an asymmetry of 0.00205 nm on the spectral bandwidth. The Appendices benchmark the computer simulation for the single-slit of various slit-widths and the symmetric double-slit with various slit-widths or slit-separations.

2. GROSS GEOMETRY OF THE DOUBLE-SLIT FOR COMPUTER SIMULATION

The goal of this work is to use computer simulation applying the Huygens–Fresnel principle to assess how an asymmetry of a double-slit would alter the interference fringe patterns. Toward that end, it becomes imperative to first evaluate the computer simulation methodologies for a single-slit with various slit widths to validate that the simulation accurately produces the known quantitative patterns of diffraction as a function of the slit-width at a given slit-to-screen distance. Further it becomes necessary to evaluate the computer simulation outcomes for a symmetric double-slit at various slit widths and various slit separations to also validate that the simulation replicates the known quantitative patterns of double-slit interference as a function of either the slit-width or the slit-separation at

otherwise fixed configuration. These two aspects of validations of the computer simulation approach are presented as the Appendices. The computer simulation is then applied to an asymmetric double-slit to assess which kind of asymmetry could have caused the interference fringe change as was reported by Radin et al. The computer simulation also serves to cross-verify the model results of Radin et al. based on the Fraunhofer far-field approximation.

The gross geometry of the double-slit to be configured to have a single aspect of asymmetry is illustrated in Figure 1. The following describes the setting of the baseline symmetric double-slit. Two slits of the widths of $2b = 10 \mu\text{m}$ are placed symmetrically with respect to a center that is located at a distance of l from a plane of observation that is parallel to the plane containing the two slits. An optical axis bisecting the double-slit is perpendicular to the observing plane. The two slits are spaced at a center-to-center distance of $w = 2a = 186 \mu\text{m}$ and the slit-screen distance is set as $l = 14.1 \text{ cm}$ to be consistent with the values fitted to the experimental data by Radin et al. (2012, 2013). In a Cartesian coordinate, the optical axis bisecting the double-slit is assigned the Z dimension, the direction along the slit's longer opening is assigned the Y dimension, and the direction along the slit's narrow opening or the width is assigned the X dimension. The slit is assumed to be infinitely long along the Y dimension to make the field of diffraction on the observation plane to be one-dimensional along the X dimension. The light distribution on the observing screen is assessed over a total lateral range of 21 mm along the X dimension that is centered at the Z-axis. This total lateral range of 21 mm is set to equal the total range of observation covered by the pixels of photo-electronic detectors used to register fringe patterns in the experiments of Radin et al. (3000 pixels, $7 \mu\text{m}$ per pixel). The wavelength of light is set as $\lambda_0 = 632.8 \text{ nm}$, as was used by Radin et al. and throughout the rest of this work unless otherwise specified. The light field illuminating the slit is assumed to be uniform. This baseline configuration of the symmetric double-slit thus carries the primarily geometric parameters of the experimental setup of Radin et al. An asymmetry may be introduced to the double-slit by changing one parameter of a slit while keeping the other slit unchanged. The parameters to change may include slit width, slit's lateral position, and intensity, wavelength, and bandwidth of light, among others.

The computer simulation has been programmed in MATLAB 2020a (Mathworks, Natick, MA). Computer simulation of the fringe patterns of the double-slit is realized by the following approaches of numeration. Each of the two slits in Figure 1 is discretized to 201 elements. The lateral coordinate of an n -th element of slit 1 with respect to the center of slit 1 is denoted by x_{1n} . A point on the observation

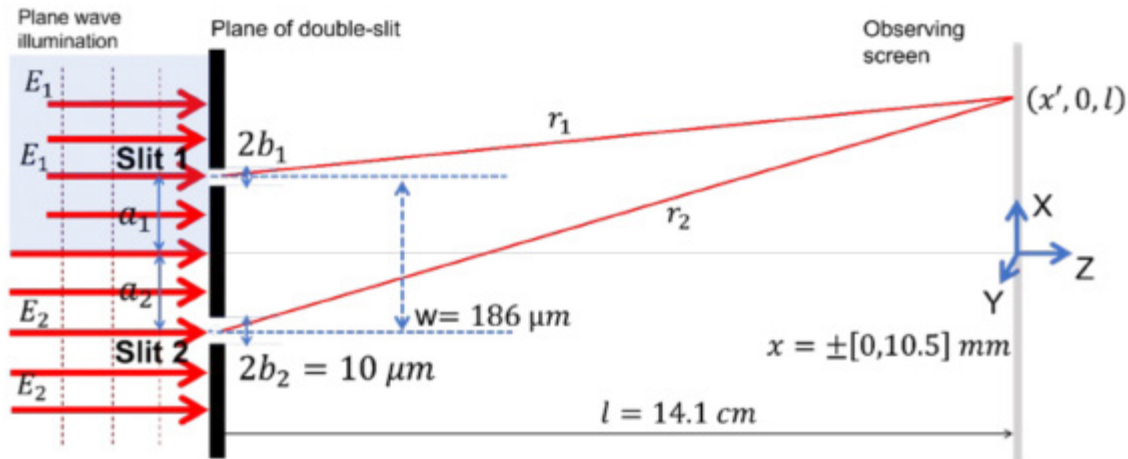


Figure 1. Schematic of a double-slit that may have one type of asymmetry for the parameters between the two slits. The symmetric baseline has a slit-separation of 186 μm , a slit-width of 10 μm , and a slit-to-screen distance of 14.1 cm. The light field on the observing screen is assessed over a total lateral range of 20 μm centered at the Z axis.

plane at a lateral distance of x' with the coordinates of $(x', 0, l)$ has an illumination distance of

$$r_{1n} = \sqrt{l^2 + (x' - a - x_{1n})^2} \quad (1)$$

from the n -th element of slit 1. Assuming that slit 1 is on the iso-phase-front of a planar wave of a field intensity of E_{10} , all differential elements of the slit then act as sources of identical strength. The complex electrical field of light at x' , originating from the differential source element x' , is

$$E_{1n}(x', 0, l, x_{1n}) \propto E_{10} \frac{1}{r_{1n}} \exp(jk_0 r_{1n}). \quad (2)$$

Likewise, the lateral coordinate of an n -th element of slit 2 with respect to the center of slit 2 is denoted by x_{2n} . Assuming that slit 2 is on the iso-phase-front of a planar wave of a field intensity of E_{20} , a point on the observation plane at a lateral distance of x' , with the coordinates of $(x', 0, l)$, has an illumination distance of

$$r_{2n} = \sqrt{l^2 + (x' + a - x_{2n})^2} \quad (3)$$

from the n -th element of slit 2. The complex electrical field of light originating from the differential source element x_{2n} is:

$$E_{2n}(x', 0, l, x_{2n}) \propto E_{20} \frac{1}{r_{2n}} \exp(jk_0 r_{2n}) \quad (4)$$

The composite complex electrical field of light on the point $(x', 0, l)$, by all discrete elements of both slits of the double-slit is then $E_{\text{double}}(x', 0, l) =$

$$E_{\text{double}}(x', 0, l) = \sum_{n=1}^N [E_{1n}(x', 0, l, x_{1n}) + E_{2n}(x', 0, l, x_{2n})] \propto \sum_{n=1}^N \left[\frac{E_{10}}{r_{1n}} \exp(jk_0 r_{1n}) + \frac{E_{20}}{r_{2n}} \exp(jk_0 r_{2n}) \right] \quad (5)$$

The light intensity distribution on the observing plane is then $I_{\text{double}}(x', 0, l) = E_{\text{double}}(x', 0, l) \times E_{\text{double}}^*(x', 0, l)$, which is the interference pattern registered by a photo-electronic array. A symmetric double-slit illuminated by monochromatic light may have $E_{10} = E_{20}$ in addition to equal slit-widths and symmetric slit-center with respect to the optical axis.

3. COMPUTER SIMULATION OF THE DOUBLE-SLIT WITH A SINGLE ASYMMETRY

The goal of this simulation study is to assess which kind of disruption to the symmetry of double-slit could have led to fringe pattern changes as were registered by Radin et al. We note that Radin et al. did not specifically document an experimental fringe pattern that deviated from the baseline when registered under the exclusive condition of the conjectured psychophysical influence. However, according to Radin et al., their analytical modeling of the double-slit with an unequal electrical field magnitude between the two slits at a ratio of 3:1 (1.5:0.5 over the baseline of 1:1) produced a fringe pattern close to what was measured experimentally. Figure 2 reprints with permission from the publisher the baseline fringe pattern and the altered pattern associated with the unequal electrical field of 3:1. These two fringe patterns were the model outputs of Radin et al. by using the Fraunhofer far-field approximation of the Huygens-Fresnel principle. These two patterns are displayed with the aspect ratio adjusted to make them look similar to the experimental fringes for the convenience of gross visual assessment hereafter.

As can be seen from Figure 2, the most perceivable difference between the baseline fringe pattern and the one

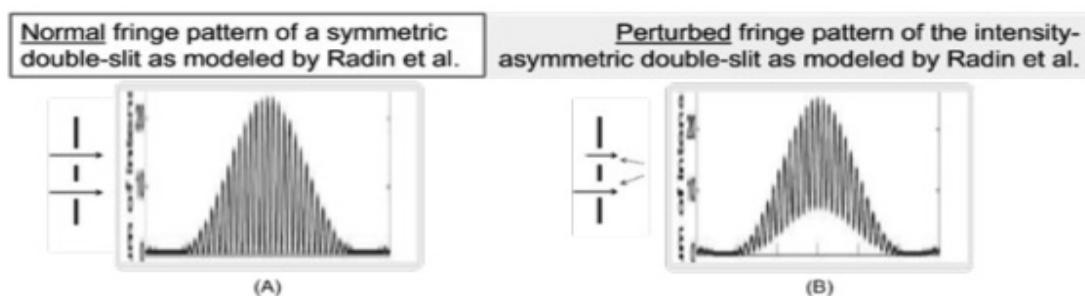


Figure 2. (A) The double-slit fringe pattern modeled by Radin et al. at normal condition when free of psychophysical influence, corresponding to a symmetric double-slit. (B) The double-slit fringe pattern modeled by Radin et al. corresponding to an asymmetry in the electrical field magnitude. Reprinted with permission.

with deviation due to unequal electrical field magnitude is the reduction of the oscillation appearing as an elevation of the lower/inner contour of the oscillating trace from the near-zero line to approximately 40% of the upper/outer contour of the oscillating trace. This reduction of the oscillatory portion over the baseline is the change of fringe visibility as was analyzed by Radin et al. An objective of the computer simulation is to find which kind of asymmetry of double-slit could produce a fringe pattern that deviates from the baseline as in Figure 2B. Any conditions of the double-slit that could lead to fringe patterns as in Figure 2B shall be given consideration in interpreting the experimental changes of the fringe under the conjectured psychophysical effects. And between two conditions leading to the similar level of fringe pattern changes in terms of the fringe visibility, the one that takes lower energy change, or equivalently smaller power, will be more likely to happen by thermal dynamic probability.

3.1. Asymmetry in the Physical Length Dimension of the Double-Slit

This section presents the simulation results of the fringe of double-slit that has one physical dimension changed from the baseline symmetric configuration. The symmetry of the physical dimensions of the double-slit is to be altered in the following aspects: an asymmetry in the slit opening, or an unequal slit width; an asymmetry in the slit offset, or a shift of one slit laterally from the baseline position of an ideally symmetric configuration.

3.1A. Asymmetry in the lateral offset of the slit-center. The effect of the slit-offset with respect to the baseline on the double-slit interference fringe pattern is illustrated in Figure 3. The asymmetry in the slit center offset is configured by changing the center of the upper slit or slit 1 with respect to the baseline position. The number of differential

elements of the slit is the same between the two slits so the total intensity of the slit would remain the same while the center of the slit is shifted laterally. The change in the fringe pattern then correlates with the asymmetry of the slit-center only. The upper panel illustrates the evolution of the asymmetry, which is to laterally shift the slit center with respect to the baseline position at a slit separation of $186 \mu\text{m}$. A lateral center-offset of slit 1 of respectively $-75 \mu\text{m}$ and $-50 \mu\text{m}$ led to a slit-separation of respectively $111 \mu\text{m}$ and $136 \mu\text{m}$, causing the geometric center of the two slits to misalign with respect to the baseline-optical axis of respectively $37.5 \mu\text{m}$ and $25 \mu\text{m}$ toward slit 2. A lateral center-offset of slit 1 of respectively $50 \mu\text{m}$ and $75 \mu\text{m}$ led to a slit-separation of respectively $236 \mu\text{m}$ and $261 \mu\text{m}$, causing the geometric center of the two slits to misalign with respect to the baseline-optical axis of respectively $25 \mu\text{m}$ and $37.5 \mu\text{m}$ away from slit 2. The upper panel illustrates the effective slit-separation caused by the lateral shift of the upper slit. The resulted fringe pattern is shown in the lower panel. The plot at the middle corresponds to the fringe pattern of a symmetric double-slit as is identical to the one in Figure 2A. None of the fringe patterns of the lower panel in Figure 3 resembles the one in Figure 2B.

The change of the fringe pattern as shown in Figure 3 can be appreciated as the following by referring to the Appendices. A change to the lateral position of one slit of the double-slit with the slit-width fixed effectively changes the slit-separation, as well as the offset of the center of the observing panel with respect to the effective center of the double-slit. The change in slit-separation causes the high-frequency pattern of the interference formed by two slits to change in frequency. The constant slit-width, however, maintains the envelope that modulates the high-frequency pattern. Reducing the lateral offset of one slit thus causes the fringe to become sparser, and conversely increasing the lateral offset of one slit makes the fringe

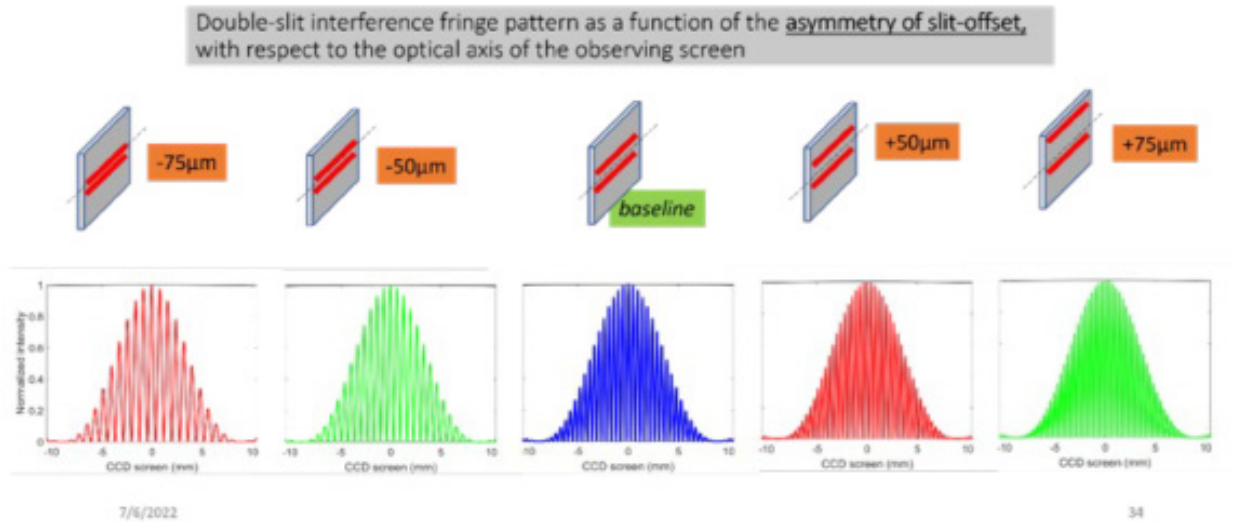


Figure 3. Double-slit interference fringe as a function of the asymmetry in geometry, specifically the offset of the slit center with respect to the baseline optical axis. **Upper panel:** The offset of the slit center, from $-75\ \mu\text{m}$, $-50\ \mu\text{m}$; baseline, $50\ \mu\text{m}$, and $75\ \mu\text{m}$. **Lower panel:** The fringe pattern corresponding to the asymmetry of slit-width.

denser, but there is no change in the envelope. As a result, the gross visibility of the fringe seems unchanged.

3.1B. Asymmetry in the slit-width of the double-slit. The effect of the asymmetry of the slit-width on the double-slit interference fringe pattern is illustrated in Figure 4. The asymmetry in the slit-width is configured by changing the width of the upper slit or slit 1 to respectively $1/5$, $1/2$, 2 times, and 5 times the baseline. The center-to-center distance, or the slit-separation, is fixed at $186\ \mu\text{m}$. The number of differential elements of the slit are the same between the two slits so the total intensity of the slit would remain the same between the two slits. The change in the fringe pattern then correlates with the asymmetry of the slit-width only. The upper panel illustrates the evolu-

tion of the asymmetry of the slit-width, from $1/5:1$ to $1/2:1$, then to baseline, then to $2:1$, and then to $5:1$. The lower panel presents the corresponding fringe pattern. The plot at the middle that corresponds to the fringe pattern of a symmetric double-slit is identical to the one in Figure 2A. None of the fringe patterns of the lower panel resembles the one in Figure 2B.

The change of the fringe pattern shown in Figure 4 is appreciable in two aspects by projecting the patterns to limiting cases while referring to the Appendices. Let's assume that one slit increases in width to overlap with the other slit. That would make the double-slit-ness disappear and the configuration essentially becomes a single-slit of a significant width of more than $186\ \mu\text{m}$. The total

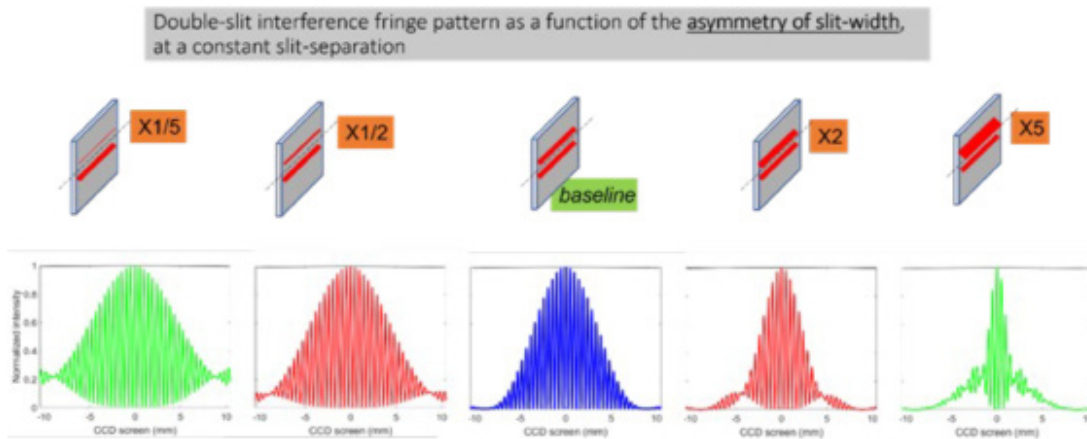


Figure 4. Double-slit interference fringe as a function of the asymmetry in the slit-width. **Upper panel:** asymmetry of the slit-width, from $1/5:1$ to $1/2:1$ to $2:1$ and $5:1$. **Lower panel:** the corresponding fringe pattern.

intensity field on the screen of observation then should be a sinc-function with a very narrow center lobe due to the large slit-width. Conversely, let's assume that the width of one slit decreases to zero. That would make the electrical field of light on the observing screen be the superposition of a double-slit of infinitely thin slit-width with a single-slit of finite width that is offset from the optical axis of the double-slit. The combined effect would cause a change in the center lobe of the fringe pattern and a change in the modulation of the lobe between the troughs.

3.2 Simulation of the Double-Slit with an Asymmetry in the Photonic Properties

This section assesses how an asymmetry of the double-slit in the photonic/spectral properties affects the interference fringe. The disruption to the asymmetry is implemented by changing one parameter of the light associated with one slit while maintaining the light associated with the other slit. The properties to be altered include the magnitude of the electrical field, the wavelength, and the spectral bandwidth of the light.

3.2A. Asymmetry in the electrical field magnitude.

Figure 5 assesses the change of the double-slit interference fringe pattern as a function of the asymmetry in the electrical field magnitude of the light between the two slits. The asymmetry in the electrical field magnitude is

configured by keeping the electrical field magnitude of the lower slit or slit 2 at the baseline and scaling the electrical field magnitude of the upper slit or slit 1 with respect to the baseline value. The total number of the discretized elements remains unchanged, and the scaling of the electrical field magnitude applies equally to all elements. The asymmetry of the electrical field magnitude is approached in two ways. The first set sets the electrical field magnitude of the light of slit 1 at respectively 1.05, 1.1, 1.5, 2, and 3 times the baseline value. The second set sets the electrical field magnitude of the light of slit 1 to respectively 1/1.05, 1/1.1, 1/1.5, $\frac{1}{2}$, and 1/3 times the baseline value. These two sets result in the same inter-slit ratio of the electrical field magnitude. The resulting fringes that are normalized with respect to their respective peak value are displayed as the upper panel in Figure 5 for the former setting and the lower panel in Figure 5B for the latter setting.

The following observations can be made with Figure 5. As the asymmetry of the electrical field magnitude between the two slits escalates, the fringe visibility degrades. However, the visibility of the normalized fringe is indifferent between the two settings with the same inter-slit ratio, regardless of which slit has the higher field magnitude. And the two fringes at the right-most, one corresponding to an asymmetry of 3:1 and the other 1/3:1, resemble Figure 2B. This result thus cross-validates the modeling of Radin et al.

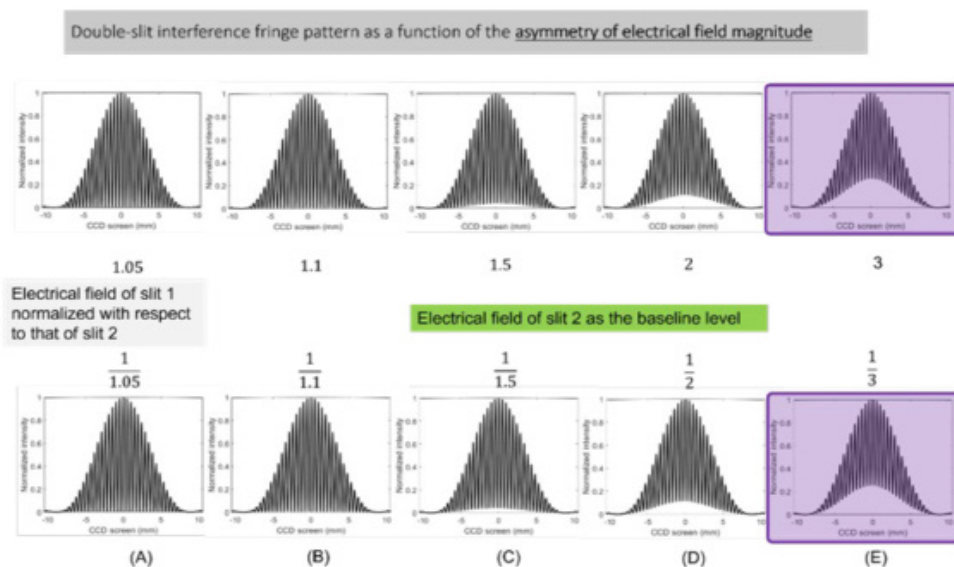


Figure 5. The change in the double-slit interference fringe pattern as a function of the asymmetry in the magnitude of the electrical field of the light. The asymmetry is configured by keeping the electrical field magnitude of one slit (the lower slit) at the baseline while scaling the electrical field magnitude of the other (the upper slit) with respect to the baseline value. The two framed plots corresponding to an asymmetry of 1:3 of the magnitude of the electrical field between the two slits are grossly different from the one in Figure 2B.

conducted by means of Fraunhofer approximation of the far-field distribution of the light field.

3.2B. Asymmetry of the slit's wavelength in the double-slit. Figure 6 compares the change of the double-slit interference fringe pattern as a function of the asymmetry of the wavelength of light. The asymmetry in the wavelength of the slit is configured by keeping the lower slit or slit 2 at baseline while changing the wavelength of the upper slit or slit 1 with respect to the baseline value (632.8 nm). The number of differential elements of the slit are the same between the two slits and so is that of the magnitude of the light field. Therefore, the only difference between the two slits is the center wavelength that changes the propagation constant to produce extra phase difference between the paths of beams originating from the two slits. The upper panel of Figure 6 illustrates the evolution of the asymmetry, as the offset of the center wavelength of slit 1 with respect to the baseline: -10 nm (622.8 nm for slit 1), -5 nm (627.8 nm for slit 1), 5 nm (637.8 nm of slit 1), and 10 nm (642.8 nm of slit 1). The corresponding fringe pattern is presented in the lower panel of Figure 6. The plot at the middle corresponds to the fringe pattern of a symmetric double-slit as is identical to the one in Figure 2A. It can be observed that the asymmetry in the wavelength of light causes the fringe oscillation to become asymmetric, even though the asymmetry does not obviously affect the fringe visibility. The asymmetry, however, may impact the frequency components when revealed by Fourier transform. But nonetheless, none of the fringe patterns of the lower panel with asymmetry in wavelength resembles the one in Figure 2B.

3.2C. Asymmetry in the spectral bandwidth of the light of the double-slit. Figure 7 presents the change of the double-slit interference fringe pattern as a function of the asymmetry of the spectral bandwidth. The asymmetry in the spectral bandwidth is configured by keeping the light properties of the lower slit or slit 2 at the monochromatic baseline while changing the bandwidth of the upper slit or slit 1. The number of differential elements of the slit are the same between the two slits and so is that of the magnitude of the light field, and the center wavelength of the light of slit 1 is 632.8 nm as is the monochromatic light of slit 2. For each of the 201 discretized elements of slit 1, it is further discretized to a total of 21 spectral elements that span over the total bandwidth as specified. And the light field of each of these 21 spectral elements is given a weight of 1/21 of that of the single element among the 201 discretized elements of slit 2. This allows the total light intensity of slit 1 with spectral broadening be the same as that of slit 2 maintained at the baseline to make the fringe change represent the effect of the spectral bandwidth only.

The two-row panel of Figure 7 going clockwise illustrates the evolution of the fringe as the spectral bandwidth of slit 1 increases from 0.001 nm, 0.004 nm, 0.01 nm, 0.1 nm, 1 nm, 2 nm, 5 nm, to 10 nm. The framed plot singled out at the left is a reprint of Figure 2B. As the asymmetry of the spectral bandwidth starts to pick up from the baseline, the fringe visibility decreases initially. The fringe visibility approaches nearly zero at 0.1 nm of the spectral bandwidth. And as the asymmetry in the spectral bandwidth increases further from 0.1 nm, the fringe visibility increases but the

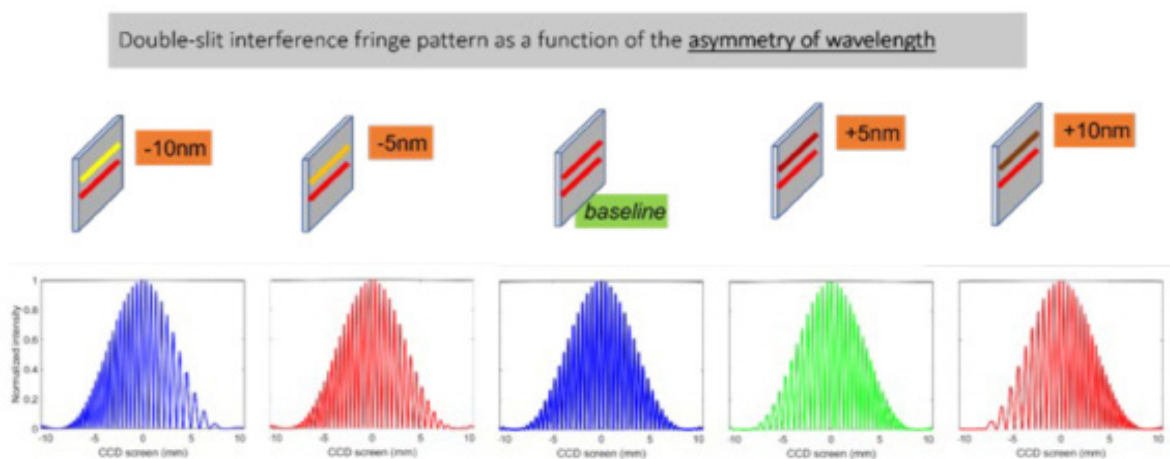


Figure 6. Double-slit interference fringe as a function of the asymmetry of the wavelength. **Upper panel:** the offset of the center wavelength, from -10nm, -5nm, baseline, 5 nm, and 10 nm. Lower panel: the fringe pattern corresponding to the asymmetry of slit-center wavelength. The plot at the middle corresponds to a symmetric double-slit identical to that in Figure 2B.

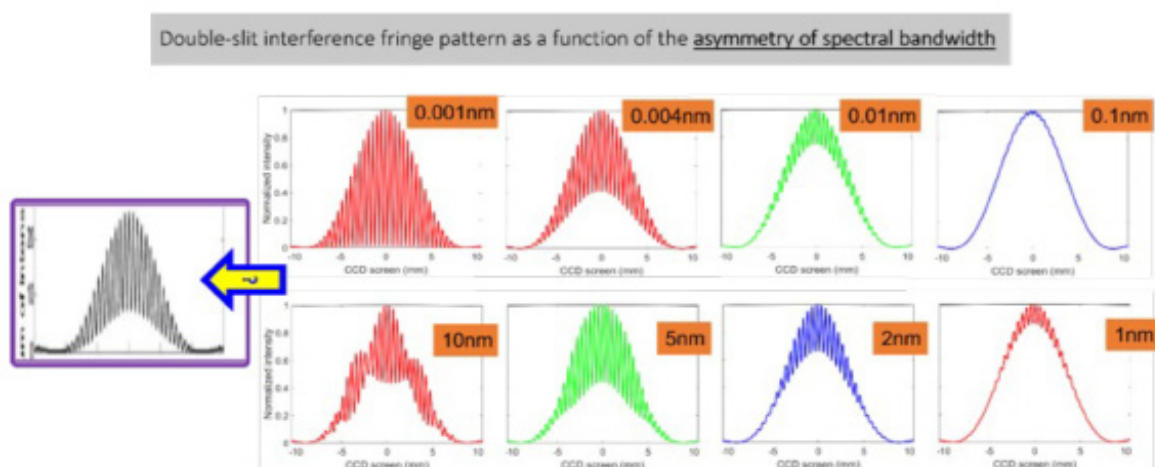


Figure 7. Double-slit interference fringe pattern as a function of the asymmetry of the spectral bandwidth. **Upper panel:** The bandwidth of the light of one slit is 0.001 nm, 0.004 nm, 0.01 nm, and 0.1 nm (in order from left to right). **Lower panel:** The bandwidth of the light of one slit is 1 nm, 2 nm, 5 nm, and 10 nm (in order from left to right). The framed plot singled out at the left (Radin et al., 2013) is reprinted with permission from *Physics Essays*.

global shape of the fringe deviates remarkably from that of the baseline. The fringe visibility of the one corresponding to the 5 nm asymmetry may be grossly analogous to that in Figure 2B, but the outer and inner contours are significantly different from those in Figure 2B. The fringe visibility of the one corresponding to the 0.004 nm asymmetry seems grossly very close to that in Figure 2B. This encourages further analysis with finer resolution in the spectral bandwidth.

3.3. Fourier Transform to Compare the Effects of Asymmetry in the Electrical Field Magnitude and the Outcomes of Asymmetry in the Spectral Bandwidth

We argue that the fringes formed by the 3:1 or 1/3:1 of asymmetry of the electrical field magnitude of light as shown in Figure 5 (the right-most pair) resemble remarkably the fringe corresponding to a 0.004 nm asymmetry in the spectral bandwidth as shown in Figure 7. We further demonstrate the analogy of the fringes formed by the two kinds of asymmetries over a greater range of the asymmetry of the electrical field magnitude and finer scale of the asymmetry of the spectral bandwidth, as shown in Figure 8. As shown in Figure 5, the fringe normalized to the center peak is grossly indistinguishable between an asymmetry of the electrical field magnitude of $\xi:1$ and that of ξ^{-1} where ξ is the inter-slit ratio of the electrical field magnitude. And in terms of the energy or power needed to change the electrical field magnitude, an asymmetry of 1/3:1 requires a 66.7% change of the light field magnitude

but an asymmetry of 3:1 requires a 200% change of the light field magnitude over the baseline. As a lower level of energy change or power is thermodynamically more plausible, in assessing the changes to the light field magnitude we chose to analyze the cases of reducing the light field magnitude of slit 1 over an increase in the light field magnitude of slit 1, given the same inter-slit ratio of the electrical field magnitude between the two slits.

Each of the sub-figures in Figure 8 contains two traces of fringe, one corresponding to an asymmetry of the electrical field magnitude and the other an asymmetry in the spectral bandwidth. For a specific level of the asymmetry of the electrical field magnitude, respectively $\frac{1}{2}:1$, $\frac{1}{3}:1$, $\frac{1}{4}:1$, $\frac{1}{5}:1$, and $\frac{1}{6}:1$, a fringe corresponding to the asymmetry of spectral bandwidth is tuned manually in the spectral bandwidth to make the two traces grossly indistinguishable based on the outer and inner contours. The traces shown correspond to an asymmetry of respectively 0.0017 nm, 0.00205 nm, 0.00223 nm, 0.0037 nm, and 0.0047 nm.

The Fourier transform of the two fringe patterns of the upper panel are displayed in the lower panel, following the same line styles (thickness and color) for the one with an asymmetry in the electrical field magnitude and the one with an asymmetry in the spectral bandwidth. Two observations can be made for the Fourier transform of the fringe patterns that are grossly indistinguishable in the fringe visibility. As the asymmetry in the electrical field magnitude increases, the shoulder of the single-slit power-peak escalates and the double-slit power reduces slightly. As the asymmetry of the spectral bandwidth intensifies, the

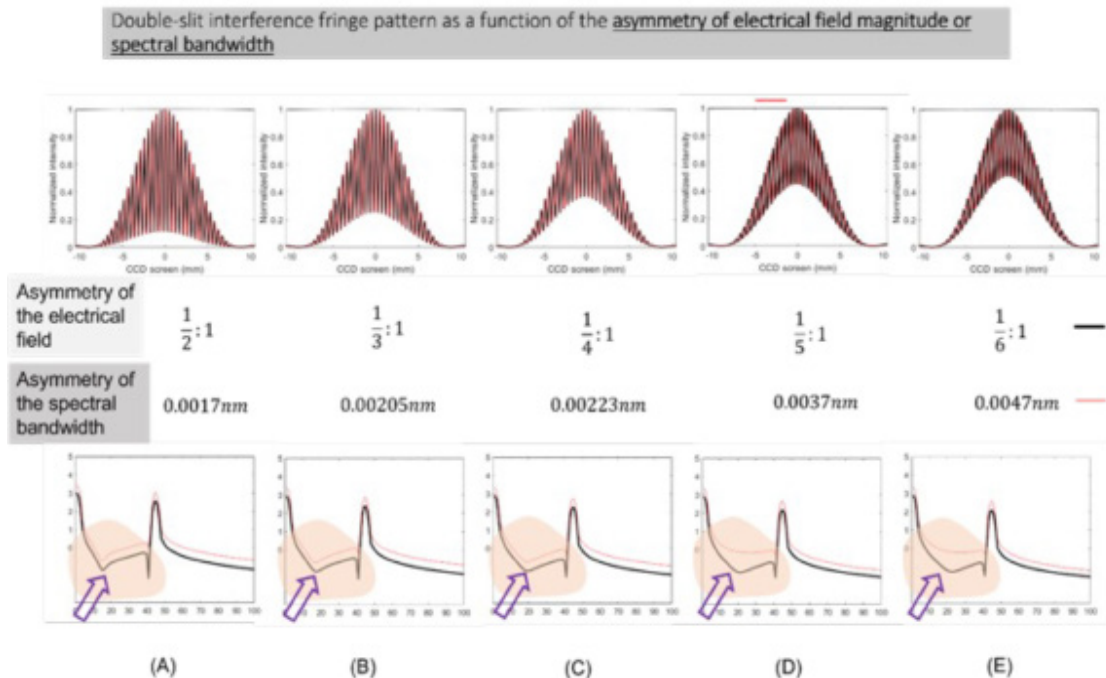


Figure 8. Upper panel: fringe patterns. The thick black fringe corresponds to an asymmetry of the electrical field magnitude and the thin red fringe corresponds to an asymmetry of spectral bandwidth. The upper and lower contours of the thick black line and thin red line are grossly identical. **Lower Panel:** the Fourier transform of the fringe pattern. The asymmetry of electrical field is 1/2:1 in (A), 1/3:1 in (B), 1/4:1 in (C), 1/5:1 in (D), and 1/6:1 in (E). The asymmetry of spectral bandwidth is 0.0017 nm in (A), 0.00205 nm in (B), 0.00223 nm in (C), 0.0037 nm in (D), and 0.0047 nm in (E).

shoulder of the single-slit power-peak elevates to a much greater extent than does the counterpart of the electrical field magnitude.

4. DISCUSSION

A double-slit in an ideal symmetric configuration leads to an interference fringe that appears as a sinusoidal carrier of 100% modulation depth with the amplitude enveloped by a squared sinc-function. The Fourier transform of the double-slit interference fringe reveals a spatial frequency component corresponding to the separation of the two slits, and a DC-bounding frequency determined by the width of the two identical slits. Any alteration to the slit-symmetry would cause a degradation of the spectral power ratio of the double-slit over single-slit from its native state corresponding to the baseline symmetry. An asymmetry between the two slits, however, could occur in various ways and therefore would not be represented only by an asymmetry in the electrical field magnitude between the two slits. As the double-slit interference is a phase-sensitive phenomenon, asymmetries in other properties of the double-slit, including spectral aspects such as the center wavelength and the spectral bandwidth, shall

not be excluded in interpreting a deviation of the interference fringe pattern from the baseline condition in the absence of a controllable or on-demand perturbation to the double-slit configuration.

What might have caused the fringe patterns in Radin's double-slit to deviate temporally from the normal condition is fundamental to the understanding of the nature of psychophysical effects that may manifest. We have demonstrated that increasing the spectral bandwidth of the light passing the slit of psychophysical intent of only 0.00205 nm at a center wavelength of 632.8 nm by keeping the same total spectral intensity to induce an asymmetry between the two slits could produce the fringe pattern changes corresponding to an asymmetry of electrical field magnitude of 1/3:1 as the replication of the modeled outcome of Radin et al. And the power spectrum of the fringe pattern corresponding to a 0.00205 nm broadening of the spectral-bandwidth of one slit seems to be noticeably closer to the experimental observation than that corresponding to a 1/3:1 inter-slit asymmetry in the electrical field magnitude. In the following, we estimate the power change that may be involved in the 0.00205 nm spectral broadening and the 1/3:1 asymmetry in the electrical field magnitude for the experimental configurations given by Radin et al.

The power change is the energy change evaluated over a given time. The energy change of light can be caused by either a number change of the photons at the same energy, or an energy change of the photons at the same total number of photons. The former corresponds to a change of the electrical field at a fixed color of the photons, and the latter corresponds to a change of the color of the photons at a fixed total number of photons.

A 3:1 inter-slit ratio of the electrical field magnitude can be configured by either a 3:1 or a 1/3:1 ratio of the electrical field magnitude between the two slits with respect to the baseline. A ratio of 3:1 of the electrical field magnitude leads to a ratio of 9:1 of the light intensity, or 800% of the change of the power with respect to baseline. A ratio of 1/3:1 of the electrical field magnitude leads to a ratio of 1/9:1 of the light intensity, or an 88.9% change in power with respect to baseline. Between these two conditions, the one that has lower power change will be more likely to happen thermodynamically, therefore we will assess the 88.9% case.

Let's assume that the number of photons amounting to the intensity of each discretized slit at the baseline is N_{total} . A reduction of the intensity to 88.9% corresponds to $88.9\% * N_{total}$ change in the number of photons associated with the discretized element of the slit. Consider that the spectral broadening of the light happens to each discretized element of the slit as the energy at a single wavelength being spread uniformly to a band of discrete wavelengths of a total number of $n_{spectral}$. The number of photons decomposed to each of the spectral composition is then $N_{total} / n_{spectral}$. A differential frequency $\Delta\nu$ over the center frequency ν_0 of light corresponds to a differential change $\Delta\lambda$ with respect to a center wavelength of λ_0 as $\frac{\Delta\nu}{\nu_0} = \frac{\Delta\lambda}{\lambda_0}$.

The differential energy (and equivalently the number of photons) of the n -th spectral decomposition over the baseline value is then $\frac{\Delta\nu_i}{\nu_0} = \frac{\Delta\lambda_i}{\lambda_0}$ where $\Delta\lambda_i = [0, \Delta\lambda_{max}]$ with $\Delta\lambda_{max}$ being one half of the total bandwidth of the spectral broadening. The total relative change of the number of photons corresponding to the entirety of the spectral decomposition for each discretized element of the slit is no greater than:

$$2 * N_{total} \left| \frac{\Delta\lambda_{max}}{\lambda} \right| = N_{total} \frac{0.00205}{632.8} = 3.24 \times 10^{-6} N_{total}. \quad (6)$$

Given that the intensity change or spectral broadening is estimated for the same resolution of discretizing the slit, the forgoing estimation leads to concluding that the spectral broadening of 0.00205 nm would take 3.64×10^{-6} times the change of photon numbers, and hence the power over the same duration of psychophysical action if incurred

needed to reach a 1/3:1 ratio of the electrical field magnitude.

It may be insightful to estimate the level of power-change corresponding to the afore-articulated 3.24×10^{-6} times the total power of the light in a slit of the double-slit of Radin et al. that would produce the fringe change comparable to that observed. According to Radin et al. (2013), a 5 mW laser passed through two 10% transmission neutral density filters would give a power illumination of 50 μ W to the double-slit 10 μ m slit width. Each slit would be placed at 100 μ m (based on the specification) from the center of the beam assuming a perfect alignment. For a collimated beam of an He-Ne laser with a cross-sectional diameter of 1 mm, assuming a top-hat beam profile, the 10 μ m slit close to the diameter of the cross-section would transmit approximately 0.63% of light, making the total power of the light passing one slit as 0.315 μ W. And 3.24×10^{-6} times this power corresponds to 1.0 pW. However, one may consider that laser beam profile is practically Gaussian, and any spectral broadening will likely be Gaussian as well which would require wider broadening to reach the same level of effect as is simulated with a uniform broadening. It may thus be safe to scale up 10 times of the power change needed to cause the expected amount of fringe visibility over what has been estimated as 1 pW, which makes 10 pW.

In the efforts to interpret the physical causes to the observed fringe pattern changes, there are perhaps two aspects of reasoning process that are consequential and not collateral, could the observed alteration to the fringe pattern changes be inexplicable by ordinary means devoid of intentional faculty. The first aspect of interpreting the observed change of the fringe patterns would be the following: Which kind of physical process could have caused that change of observation? And the second aspect of interpreting the observed change of the fringe patterns should be the following: How could the physical process indicated by the prior aspect correlate with the introduction of an intentional faculty directed to that effect? From the standpoint of energy-transformation or energy-transduction, a process that requires the lesser change of energy or power would be more likely to happen since the thermodynamic probability of an energy difference of ΔE decreases at a rate of $\exp(-\Delta E/E_t)$ where E_t is the thermal energy, should the thermal-dynamic condition not be violated. However, the question of how intentional faculty could possibly act upon a physically sensitive entity to cause a psychophysical effect being manifested is perhaps premature to be contemplated, until the most plausible physical cause or process that can account for the observed physical effects subjected to intentional faculty can be identified. Since double-slit interference is an optical phenomenon, the interpretation

of the fringe pattern deviation from a normal condition shall not prefer the intensity change over other kinds of parameter variation, as was stated by Nelson (1981): "Since the fringe position is also sensitive to the wavelength of the light source and to the index of refraction of the air between its plates, these parameters cannot be excluded as possible components in the PK interaction."

5. CONCLUSIONS

Computer simulation based on the Huygens–Fresnel principle has been implemented to assess how the double-slit interference pattern changes as the symmetry of double-slit is disrupted. We demonstrate that an asymmetry in the spectral bandwidth of the light between the two slits, specifically a 0.00205 nm uniform spectral broadening of the light at a center wavelength of 632.8 nm for one slit, can vary the fringe to have a visibility nearly indistinguishable from that due to an asymmetry of the electrical field magnitude of 1/3:1 as was modeled by Radin et al. As far as the change of energy or power is concerned, the 0.00205 nm spectral broadening of the light would take about 1/300,000th of the power of the 2/3 reduction of the electrical field magnitude of light to reach an inter-slit ratio of 1/3:1 of the electrical field magnitude, both at a center wavelength of 632.8 nm. The former one, which takes approximately 5 orders of magnitude less in power change than the latter one, could be much more plausible than the latter one. The amount of power involved in perturbing the spectral bandwidth of 0.00205 nm in the experimental setting of Radin et al. is estimated to be no more than 10 pW. The level of energy transformation or transduction pertinent to psychophysical intent may be worthy of experimental examination.

IMPLICATIONS AND APPLICATIONS

This study has challenged the interpretation of the physical cause of the fringe pattern changes in the double-slit experiments of Radin et al., revealing neurophysiological correlation with intentioned influence. Finding an alternative interpretation to the effect that takes just about 3.64×10^{-6} of the power of that modeled by Radin et al. is expected to open a new avenue for experimental approaches to target any energy-associative mechanism of psychophysical effects.

ACKNOWLEDGMENTS

This manuscript is based upon a full-member workshop the author presented to the Society of Scientific Exploration on December 10, 2021. The author thanks the audiences of that workshop including Dr. Dean Radin for

their insightful discussions.

Data-sharing Plan. The computer programs in MATLAB are available to share upon reasonable requests to the author.

Author Contributions. The author is solely responsible for conceptualization, methodology, execution, and writing of this manuscript.

REFERENCES

- Alexander, K. (2019). A multi-frequency replication of the MegaREG experiments. *Journal of Scientific Exploration*, 33, 435–450. [10.31275/2019/1278](https://doi.org/10.31275/2019/1278).
- Ambrose, B. S., Shaffer, P. S., Steinberg, R. N., & McDermott, L. C. (1999). An investigation of student understanding of single-slit diffraction and double-slit interference. *American Journal of Physics*, 67(2), 146–155. [10.1119/1.19210](https://doi.org/10.1119/1.19210)
- Bierman, D. J. (1996). Exploring correlations between local emotional and global emotional events and the behavior of a random number generator. *Journal of Scientific Exploration*, 10, 363–373. https://www.scientificexploration.org/docs/10/jse_10_3_bierman.pdf
- Dunne, B. J., & Jahn, R. G. (1992). Experiments in remote human/machine interaction. *Journal of Scientific Exploration*, 6, 311–332. <https://doi.org/10.1016/j.explore.2007.03.025>
- Gachet, D., Brustlein, S., & Rigneault, H. (2010). Revisiting the Young's double-slit experiment for background-free nonlinear Raman spectroscopy and microscopy. *Physical Review Letters*, 104(21), 213905. <https://doi.org/10.1103/PhysRevLett.104.213905>
- Giroldini, W., & Pederzoli, L. (2021). EEG activity during mental influence on a random signal generator. *Journal of Scientific Exploration*, 35, 267–286. [10.13140/RG.2.2.25130.85444](https://doi.org/10.13140/RG.2.2.25130.85444)
- Jahn, R. G. (1982). The persistent paradox of psychic phenomena: An engineering perspective. *Proceedings of the IEEE*, 70, 136–170. [10.1109/PROC.1982.12260](https://doi.org/10.1109/PROC.1982.12260)
- Jamali, M., Golshani, M., Jamali, Y. (2019). A proposed mechanism for mind–brain interaction using extended Bohmian quantum mechanics in Avicenna's monotheistic perspective. *Heliyon*, 5(7), e02130. <https://doi.org/10.1016/j.heliyon.2019.e02130>
- Klein, S. A., & Cochran, C. (2017). Physics and the role of mind. AIP Conference Proceedings. <https://aip.scitation.org/doi/pdf/10.1063/1.4982778>
- Lee, K., Lim, J., & Ahn, J. (2013). Young's experiment with a double-slit of sub-wavelength dimensions. *Optics Express*, 21(16), 18805–18811. <https://doi.org/10.1364/OE.21.018805>
- McConnell, R. A. (1989). Psychokinetic data structure.

- Journal of the American Society for Psychical Research*, 88, 217. <https://psycnet.apa.org/record/1990-21351-001>
- Nelson, R. D., Dunne, B. J., & Jahn, R. G. (1981). Psychokinesis studies with a Fabry-Perot interferometer. *Research in Parapsychology*, 47–50.
- Piao, D. (2021). Could the sheep-goat effect be the manifestation of attentional-phase dependent mind-matter modulation? *Physics Essays*, 34(3), 297–314. 10.4006/0836-1398-34.3.297
- Pratt, J. G. (1949). The meaning of performance curves in ESP and PK test data. *Journal of Parapsychology*, 13, 9–23. <https://pubmed.ncbi.nlm.nih.gov/18114579/>
- Radin, D. I. (1982). Experimental attempts to influence pseudorandom number sequences. *Journal of the American Society for Psychical Research*, 76, 359–374.
- Radin, D., Michel, L., Galdamez, P., Wendland, R., Rickenbach, R., & Delorme, A. (2012). Consciousness and the double-slit interference pattern: Six experiments. *Physics Essays*, 25, 157–171. 10.4006/0836-1398-25.2.157
- Radin, D., Michel, L., Johnston, J., & Delorme, A. (2013). Psychophysical interactions with a double-slit interference pattern. *Physics Essays*, 26, 553–556. 10.4006/0836-1398-34.1.79
- Radin, D., Michel, L., & Delorme, A. (2016). Psychophysical modulation of fringe visibility in a distant double-slit optical system. *Physics Essay*, 29(1), 14–22. 10.4006/0836-1398-29.1.014
- Rhine, L. E. (1963). Spontaneous physical effects and the psi process. *Journal of Parapsychology*, 27, 84–122.
- Schmidt, H. (1973). PK tests with a high-speed random number generator. *Journal of Parapsychology*, 37, 105–118.
- Shewmaker, K. L., & Berenda, C. W. (1962). Science and the problem of psi. *Philosophy of Science*, 29(2), 195–203.
- Sztul, H. I., & Alfano, R. R. (2006). Double-slit interference with Laguerre-Gaussian beams. *Optics Letters*, 31(7), 999–1001. 10.1364/ol.31.000999
- Tart, C. T., Puthoff, H. E., & Targ, R. (1980). Information transmission in remote viewing experiments. *Nature*, 284(5752), 191. 10.1038/284191a0
- Thompson, B. J., & Wolf E. (1957). Two-beam interference with partially coherent light. *Journal of The Optical Society of America*, 47(10), 895–902. <https://doi.org/10.1364/JOSA.47.000895>
- Tremblay, N. (2019). Independent re-analysis of alleged mind-matter interaction in double-slit experimental data. *PLOS ONE*, 14(2), e0211511. 10.1371/journal.pone.0211511
- Utts, J. M. (1986). "he Ganzfeld debate: A statistician's perspective. *Journal of Parapsychology*, 50, 393–402. <https://psycnet.apa.org/record/1988-12545-001>
- Walleczek, J., & von Stillfried, N. (2019). False-positive effect in the Radin double-slit experiment on observer consciousness as determined with the advanced meta-experimental protocol. *Frontiers in Psychology*, 10, 1891. <https://doi.org/10.3389/fpsyg.2019.01891>
- Yacoby, A., Heiblum, M., Umansky, V. V., Shtrikman, H., & Mahalu, D. (1994). Unexpected periodicity in an electronic double-slit interference experiment. *Physical Review Letters*, 73(23), 3149–3152. <https://doi.org/10.1103/PhysRevLett.73.3149>
- Young, T. (1804). The Bakerian lecture. Experiments and calculation relative to physical optics. *Philosophical Transactions of the Royal Society of London*, 94, 1–16.

APPENDICES

Double-slit interference as a classical wave optical phenomenon has been known for more than 2 centuries (Young, 1804) and surrenders to accurate analysis by way of the standard wave approaches such as the Huygens–Fresnel principle which becomes Fraunhofer approximation at the far-field limit. The Huygens–Fresnel principle treats the light field from an aperture as the superposition of the light field originating from all differential elements of the aperture, each of which is treated as a point source of light radiation. And the light intensity as is registered on an observation plane is the product of the complex electrical field and the conjugate of that complex electrical field. The textbook analysis of double-slit interference usually attends to symmetrically configured double-slit (Ambrose et al., 1999). And analytical approaches that may be implemented straightforwardly for numerical evaluation have seldom treated the double-slit with an asymmetry and thus do not offer the flexibility of assessing the effect of various kinds of asymmetry on the fringe pattern as is needed for this work.

The goal of this work is to use computer simulation operations of the Huygens–Fresnel principle to assess how the asymmetry of double-slit would alter the interference fringe patterns to understand the possible physical causes or precursors to the changes in fringe visibility of double-slit as reported by Radin et al. The implementation of computer simulation based on the Huygens–Fresnel principle should facilitate arbitrary asymmetry configuration between the two slits. It is noted that the slit practically has a finite width even though the length of the slit may be idealized as being infinite. Unlike analytical treatment that can deal with the differential elements of a slit by integrating over the entirety of the slit-width, computer simulation must discretize a slit along the width and sum up the contributions from all those discrete elements. It thus becomes imperative to benchmark the performance of the computer simulation against the results known for

symmetric double-slit (Thompson & Wolf, 1957), prior to applying the computer simulation to an asymmetric double-slit to study the effect of each kind of asymmetry on the fringe pattern.

The spatial distribution of light field impinging on a symmetric double-slit can be treated as the spatial distribution of the light field impinging on a single-slit which has a width identical to each double-slit, convolving with the spatial distribution of the centers of the two slits. Since the radiation pattern of a source is mathematically proportional to the spatial Fourier transform of the source profile, the double-slit interference fringe is essentially a multiplication between the radiation pattern by a double-slit of infinitely small slit-width with the spatial Fourier transform of the single-slit's width function—a rectangular distribution for an ideal slit. Any change to the fringe pattern of a symmetric double-slit can thereby be understood effectively by assessing the overlay between a radiation pattern (square of a sinc-function) characteristic of a single-slit and a spatial pattern (oscillation) inherent to a double-slit of infinitely thin slit-width.

Toward that end, we first evaluate the computer simulation for a single-slit with various slit widths to validate that the simulation produces accurately the known quantitative patterns of diffraction as a function of the slit-width at a given slit-to-screen distance. We then evaluate the computer simulation for a symmetric double-slit at various slit widths and various slit separations to also validate that the simulation produces accurately the known quantitative patterns of double-slit interference as a function of either the slit-width or the slit-separation at otherwise fixed configuration. The computer simulation validated for single-slit and symmetric double-slit will then be applied

to double-slit configured with an asymmetry to assess which kinds of asymmetry could be relevant to the changes of interference fringe pattern reported by Radin et al. The computer simulation also serves to cross-examine the results of Radin et al. modeled with the Fraunhofer far-field approximation, which is the limiting case of the Huygens–Fresnel principle.

Appendix A. Validation of the Computer Simulation for Single-Slit at Various Slit Widths

We first establish a computer simulation based on the Huygens–Fresnel principle to produce the mundane pattern of single-slit diffraction. This step for validation serves to assure that the effect of the single-slit parameters on the light field on the observing screen of the double-slit is handled correctly. Meanwhile, this step would also help us visualize how the physical dimensional parameters of each of the two slits of equal width in the double-slit would affect the interference fringe pattern since the envelope that modulates the oscillation caused by the separation of the two slits in double-slit is controlled by the width of the two slits of equal width.

Appendix A1. Configuration of the single-slit for computer simulation. The geometric configuration of the single-slit used to validate the computer simulation approach of this work is illustrated in Figure A1. The slit of width $2b$ is placed at an axial distance of λ from a plane of observation that is perpendicular to the optical axis of the single-slit. The slit-screen distance is set as $\lambda = 14.1$ cm to make it consistent with the slit-to-screen distance in the double-slit experiment of Radin et al. (2012, 2013).

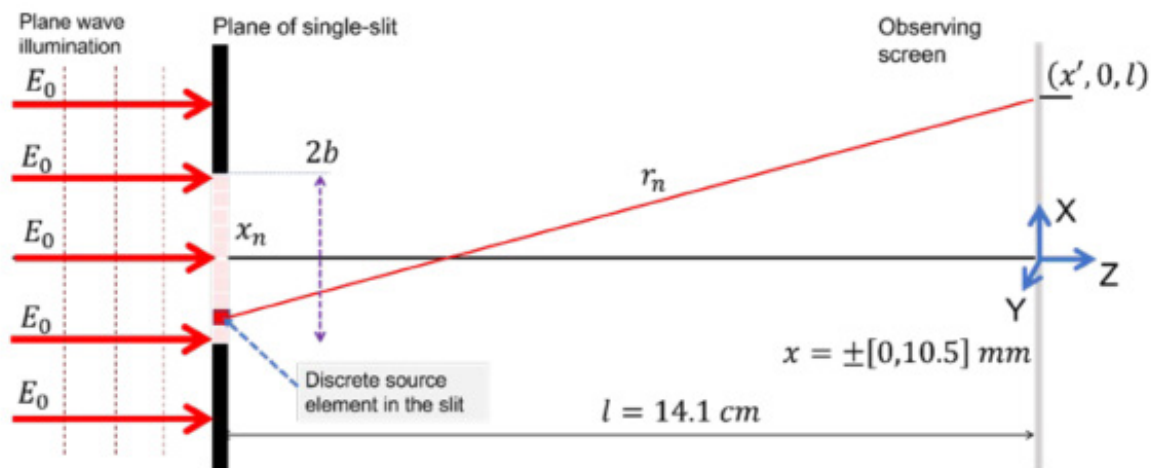


Figure A1. Schematic of single-slit configuration with the slit-to-screen distance and screen-size the same as those of the double-slit of Radin et al. (2013). The slit-width is denoted as $2b$. The slit-to-screen distance is 14.1 cm. The light field on the observation plane is assessed over a total lateral range of 21 mm symmetric to the optical axis that dissects the slit opening.

In a Cartesian coordinate, the optical axis bisecting the single-slit is assigned the Z dimension, the direction along the slit's longer opening is assigned the Y dimension, and the direction along the slit's narrow opening or the width is assigned the X dimension. The slit is assumed to be infinitely long along the Y dimension to make the field of diffraction on the observation plane one dimensional along the X dimension. The light distribution on the observing screen is assessed over a total range of 21 mm along the X dimension, or a bilateral range of 10.5 mm with respect to the Z-axis. This total lateral range of 21 mm is set to equal the total range of observation covered by the pixels of photo-electronic detectors used to register fringe-patterns in the experiments of Radin et al. (3000 pixels, 7 μm per pixel). The wavelength of light is set as $\lambda_0 = 632.8 \text{ nm}$.

According to the Huygens–Fresnel's principle, each differential element of an aperture is treated as a point source from which the light irradiates spherically. The single-slit is discretized to a total of n elements. The lateral position of the n -th element with respect to the slit center is denoted as x_n . A point on the plane of observation at a lateral distance of x' at the coordinates of $(x', 0, l)$ has an illumination distance of:

$$r_n = \sqrt{l^2 + (x' - x_n)^2} \quad (\text{A1})$$

from the n -th differential element on the slit. Assuming that the single-slit is on the iso-phase-front of a planar wave with an electrical field magnitude of E_0 , then all differential elements of the slit act as sources of identical strength. The electrical field of light impinging on

the observing plane and originating from a differential source element x_n is:

$$E_n(x', 0, l, x_n) \propto \frac{E_0}{r_n} \exp(jk_0 r_n), \quad (\text{A2})$$

where $k_0 = 2\pi/\lambda_0$ is the monochromatic propagation constant. The composite electrical field of the light on the point of observation of $(x', 0, l)$ originating from all discrete elements of the single-slit is

$$E_{\text{single}}(x', 0, l) = E_{\text{single}}(x', 0, l) = \sum_{n=1}^N E_n(x', 0, l, x_n) \propto \sum_{n=1}^N \frac{E_0}{r_n} \exp(jk_0 r_n). \quad (\text{A3})$$

The corresponding light intensity is then $I_{\text{single}}(x', 0, l) = E_{\text{single}}(x', 0, l) \cdot E_{\text{single}}^*(x', 0, l)$, which is the diffraction pattern of the single-slit that is actually registered by a photo-electronic array.

Since computer simulation using the Huygens–Fresnel principle cannot circumvent discretizing the slit into elements, the resolution of the discretization will affect the accuracy of modeling the light field on the plane of observation. It can be expected that the accuracy of modeling the light field on the plane of observation will improve as more elements are discretized over the slit. It can also be projected that as the number of discretized elements of the slit reaches a certain value, further increase will not indifferently change the composite light field after the contribution by all elements saturates. This work found it adequate to discretize the single-slit or each of the two slits of the double-slit to 201 elements.

Appendix A2. Diffraction patterns simulated for a

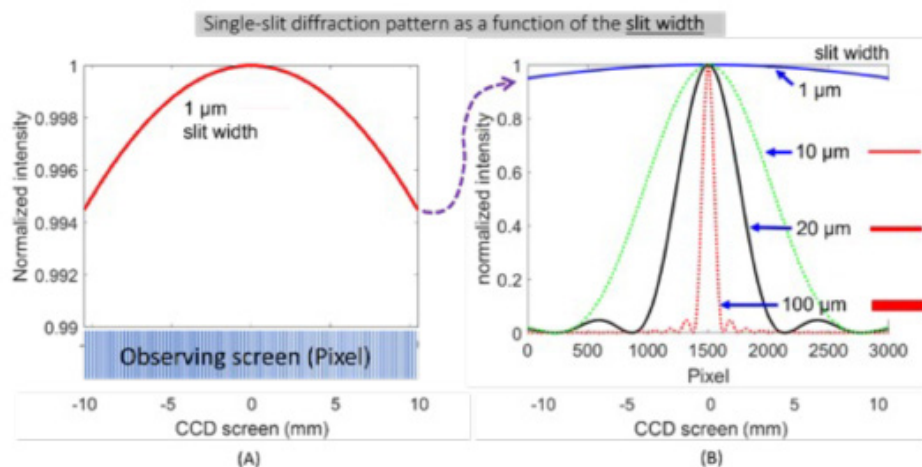


Figure A2. (A) The intensity of the diffracted field over a 21 mm span at a distance of 14.1 cm from a single-slit of 1 μm . The total 3000 pixels of the photo-electronic (denoted as CCD screen for convenience) array covers a 21 mm range or a $[-10.5, 10.5]$ mm range. The intensity of the diffraction field drops to $\sim 99.45\%$ at the edge of the observing range when compared to that at the center. (B) The evolution of the single-slit diffraction pattern as the slit-width increases. The slightly curved line atop the others is associated with a single-slit of 1 μm slit-width as is given in (A). The other curves are associated with slit-width of 10 μm , 20 μm , and 100 μm , at the order of reduced width of the center lobe.

single-slit at various slit widths. Figure A2 displays the simulated light intensity on the observing plane of the single-slit shown in Figure A1. The slit-width is set as one of the following: 1 μm , 10 μm , 20 μm , and 100 μm , respectively. Figure A1A corresponds to a slit-width of 1 μm and has the ordinate zoomed in to illustrate the small reduction of the light intensity ($\sim 0.55\%$ reduction) toward the edge of the observing range with respect to that of the maximum at the center. Figure A2B displays how the single-slit diffraction pattern varies as the slit-width increases. The slightly curved line atop the others is the duplication of the one in Figure A2A that is associated with a slit-width of 1 μm . The other curves correspond to the diffraction patterns associated with slit widths of respectively 10 μm , 20 μm , and 100 μm , at the order of reduced width of the center lobe.

The spatial intensity distribution of a single-slit is equivalent to a line source convolved with a rectangular function characterizing the slit-width. The diffraction pattern of a single-slit is therefore the irradiation pattern of a line source multiplied with the Fourier transform of the rectangular function representing the slit width which is a sinc-function. The resulted diffraction pattern of single-slit, the intensity profile registered along the X dimension or along a direction orthogonal to the line opening of the slit, thus carries an envelope as shown in Figure A2B that is slightly modified over the square of a sinc-function (the slight modification is due to the slightly varying distance of the field point on the observing plane to the slit center) as is characterized by the lobes separated by the regularly spaced zero-reaching minima. The zero-reaching minima on each later side of the center point occur at lateral positions that are spaced at a constant interval of $\lambda_0 \frac{l}{2b}$.

With the rest of the slit parameters fixed, the spacing between the minima is scaled inversely over the slit width. The center lobe for the 20 μm is 1/2 the width of the 10 μm slit. And the first zero position of the 100 μm slit is 10 times smaller than that of the 10 μm slit.

Appendix B. Fringe Pattern Simulated for a Symmetric Double-Slit with Various Slit Widths and Slit Separations

We then establish computer simulation based on the Huygens–Fresnel principle in producing the mundane interference fringe pattern of a symmetric double-slit and the salient features of double-slit in relating to single-slit pattern. The geometry of a symmetric baseline of the double-slit used to further validate the computer simulation approach is referred to in Figure 1.

Appendix B1. Effect of the slit separation on the interference fringe of a symmetric double-slit at a fixed infinitely thin slit-width. The interference fringe of the symmetric baseline of the double-slit referred to in Figure 1 is assessed for the dependence on the slip separation at the infinitely narrow slit-width. The results are shown in Figure A3 for three values of the slit separation, 1 μm (the thin blue line that is slightly curved), 10 μm (the thick black line that has approximately 2.5 cycles in the field of view), and 186 μm (the thin red line that is much denser in oscillation than the other two profiles). The infinitely narrow slit-width would make the double-slit interference fringe free of the effect of the slit-opening and thereby represent only the spatial frequency characteristics due to separation of the two slits. The fringe makes a 2π phase change over a

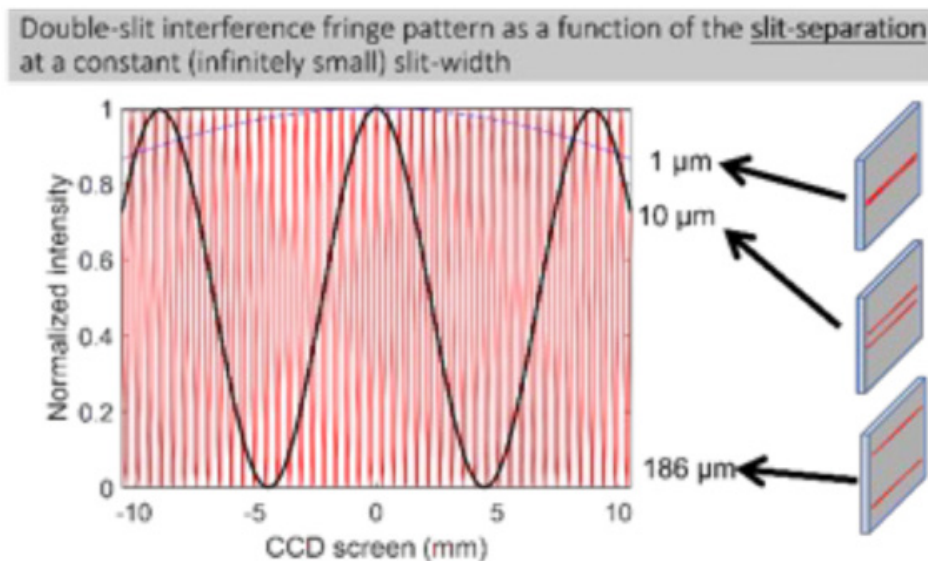


Figure A3. Illustration of how the slit-separation of a double-slit affects the interference fringe. The slit-width is set as infinitely thin. The three curves correspond to three values of slit separation, 1 μm , 10 μm , and 186 μm , respectively.

lateral distance of $\lambda_0 \frac{l}{w}$. As the slit separation w increases, the spatial distance for the fringe to make a 2π phase change becomes smaller, causing a denser cycle or higher spatial frequency of the light intensity distribution on the observing plane.

Appendix B2. Effect of the slit-width on the interference fringe pattern of a symmetric double-slit at a fixed slit separation. The interference fringe of the symmetric baseline of the double-slit referred to in Figure 1 is assessed for the dependence on the slit-width at a constant slit-separation of $186 \mu\text{m}$. The results are given in Figure A4 at four values of the slit width, $0 \mu\text{m}$ (the thin red cycles barely seen at both of the upper corners), $1 \mu\text{m}$ (the thin black cycles whose amplitude is tapered slightly at both of the upper corners), $5 \mu\text{m}$ (the thicker green cycles whose amplitude is tapered significantly toward both lateral aspects), and $10 \mu\text{m}$ (the thickest blue cycles whose amplitude is tapered with a trough appearing toward both lateral aspects). The line of $0 \mu\text{m}$ slit-width at this fixed slit-separation of $186 \mu\text{m}$ in Figure A4 is identical to the line of $186 \mu\text{m}$ slit-separation with the slit-width being infinitely thin as in Figure A3.

As is indicated by Figure A4, keeping the slit-separation constant keeps the spatial frequency representing the cycling of the fringe pattern unchanged, thereby any change to the fringe pattern will represent the effect of the slit-width. By referring to Figure A2 for the effect of the slit-width, one can see that increasing the slit-width will make narrower the envelope modulating the cycling representing the constant spatial frequency of the separation

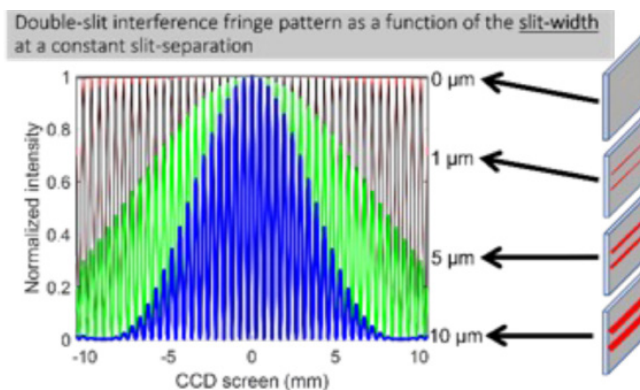


Figure A4. Illustration of how the slit-width of a double-slit affects the interference fringe. The slit-separation is set at a constant value of $186 \mu\text{m}$. The four traces correspond to four values of slit-width, $0 \mu\text{m}$, $1 \mu\text{m}$, $5 \mu\text{m}$, and $10 \mu\text{m}$, respectively.

between the two slits.

The combined effect of a finite width of the slit and the slit-separation of a symmetric double-slit on forming the fringe pattern at the observational plane is illustrated in Figure A5 for the specific configuration of a slit-width of $10 \mu\text{m}$ and a slit separation of $186 \mu\text{m}$. As shown in Figure A5A, the dense cycle represents the spatial frequency of double-slit that is proportional to the inversion of the center-to-center distance between the two slits, and the dashed line with a bell-shaped lobe corresponds to the spatial intensity distribution determined by the width of single-slit. The multiplication of the two types of patterns leads to the one in Figure A5B, a fast cycle with the ampli-

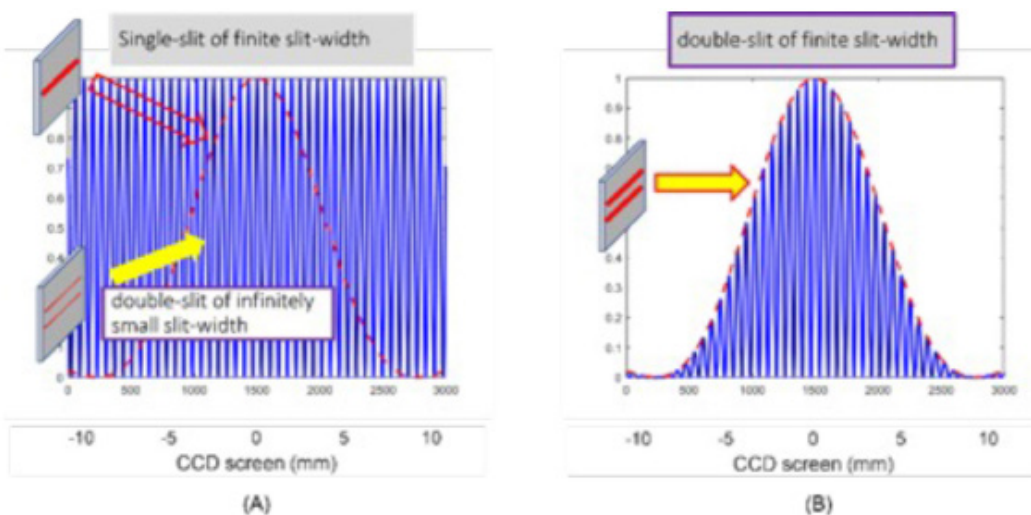


Figure A5. The interference fringe of a double-slit of finite slit-width is the enveloping of the amplitude of an oscillation by the spatial pattern of diffraction determined by the width of the single-slit. **(A)** The high-frequency blue trace of iso-amplitude is characteristic of the spatial separation of the two slits. The dashed red line corresponds to the single-slit diffraction. **(B)** The double-slit interference fringe is the outcome of the slit-separation mandated oscillation modulated in amplitude by the single-slit determined diffraction pattern.

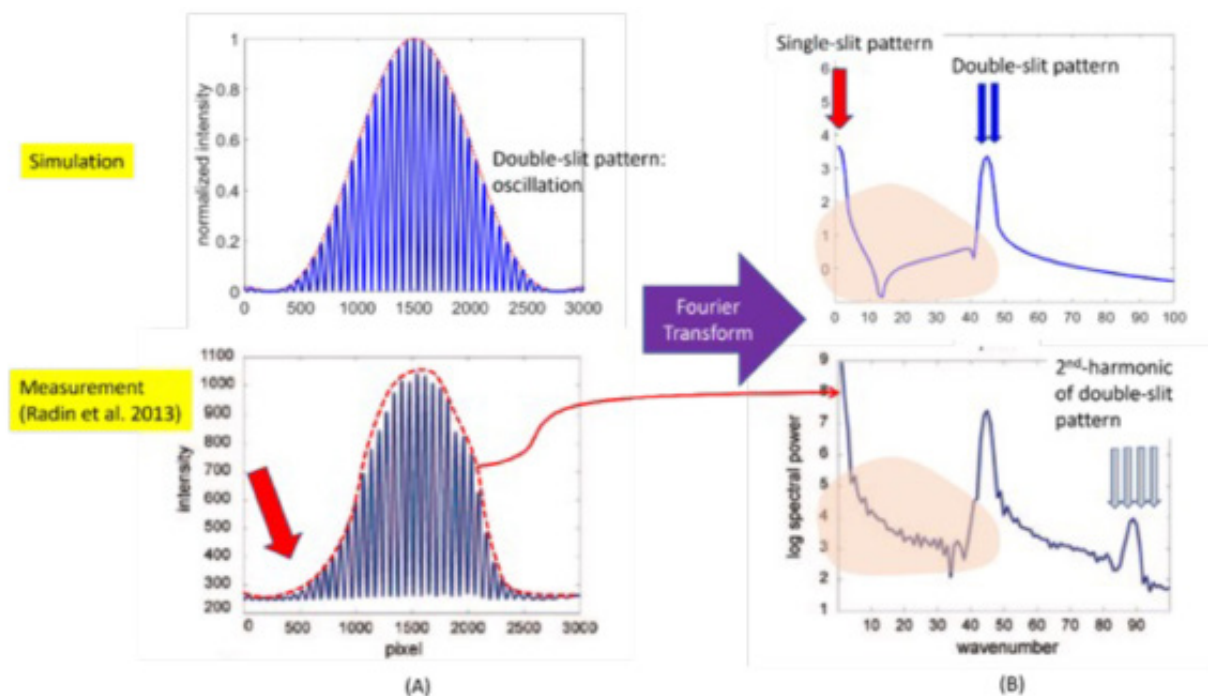


Figure A6. Upper panel: Computer simulation of the interference fringe pattern of a symmetric double-slit, identical to that in Figure A5B. The fringe pattern with the envelope marked with a dashed red line is in the left column and the Fourier transform of the fringe pattern is in the right column. **Lower panel:** experimental interference fringe pattern of the double-slit of Radin et al. The envelope marked with a dashed line is asymmetric, which was caused by a slight misalignment of the slit-center versus the center of the photo-electronic array, according to Radin et al.

tude enveloped by a slow symmetric function of the square of the sinc-function as the double-slit fringe.

Appendix B3. Comparing the computer-simulated fringe pattern of the symmetric double-slit and its Fourier transform against the experimental results of Radin et al. The validity of computer simulation approaches the symmetric baseline of the double-slit referred to in Figure 1 that has the same primary physical parameters as that of Radin et al. can be appreciated by comparing the simulated fringe against the experimental recording of Radin et al. Figure A6 presents both the double-slit fringe pattern and its Fourier transform in reference to the respective experimental results of Radin et al. (reprinted with permission). The upper panel contains computer simulation results, and the lower panel corresponds to experimental results. The fringe patterns are compared on column (A) between computer simulation and experimental registration. The power spectra are compared in (B) between the Fourier transform of computer simulated fringe pattern and the Fourier transform of the experimental data as reported by Radin et al.

We note that the simulated fringe pattern grossly matches that of experimental registration in terms of the shape of the envelope and the oscillation frequency. The match of the computer simulation with the experimental registration of the fringe pattern can be further appreciated by comparing their respective Fourier transformations shown in the right column of Figure A6. The Fourier

transform of the simulated fringe has a DC-bounding peak pointed to by the single framed red arrow, and another peak to the right that is pointed to by the two framed blue arrows. These two peaks align with the corresponding peaks of the Fourier Transform of the experimental fringe which has another peak of higher frequency but lower power as was pointed to by the four framed grey arrows. As was specified by Radin et al., the peak marked by the two framed blue arrows represents the oscillation caused by the separation of the two slits and therefore the double-slit power. The DC-bounding peak marked by the single framed red arrow corresponds to the width of the slit and thereby the single-slit power. The experimentally registered fringe becomes slightly asymmetric, causing the 2nd harmonic of the double-slit pattern to show up in the Fourier transform. The asymmetric distortion of the experimental fringe was also found by Radin et al. to indicate a slight misalignment between the double-slit and the photo-detector array as well as a slightly unequal width between the two slits. These non-ideal conditions and a baseline noise level of the photo-detection might also have caused the elevation of the shoulder of the single-slit power in the Fourier transform of the experimental data. Comparatively, in the computer simulation to which no baseline noise was added and where the double-slit has been ideally symmetric and aligned, the Fourier transform shows clean profiles of a double-slit power and a single-slit power.